ISBN: 978-3-95450-232-5 ISSN: 2673-7000 doi:10.18429/JACoW-NAPAC2022-MOZD4

UNCERTAINTY QUANTIFICATION OF BEAM PARAMETERS IN A LINEAR INDUCTION ACCELERATOR INFERRED FROM BAYESIAN ANALYSIS OF SOLENOID SCANS*

M. A. Jaworski, D. C. Moir, S. Szustkowski
Los Alamos National Laboratory, Los Alamos, NM, USA

Abstract

Linear induction accelerators (LIAs) such as the DARHT at Los Alamos National Laboratory make use of the beam envelope equation to simulate the beam and design experiments. Accepted practice is to infer beam parameters using the solenoid scan technique with optical transition radiation (OTR) beam profiles. These scans are then analyzed with an envelope equation solver to find a solution consistent with the data and machine parameters (beam energy, current, magnetic field, and geometry). The most common code for this purpose with flash-radiography LIAs is xtr. The code assumes the machine parameters are perfectly known and that beam profiles will follow a normal distribution about the best fit and solves by minimizing a χ^2-*like* metric. We construct a Bayesian model fo the beam parameters allowing maching parameters, such as solenoid position, to vary within reasonable uncertainty bounds. Posterior distribution functions are constructed using Markov-Chain Monte Carlo (MCMC) methods to evaluate the accuracy of the xtr solution uncertainties and the impact of finite precision in measurements.

INTRODUCTION

Without some quantification of uncertainties in the measurement and analysis of experiments, model differentiation becomes difficult or impossible. In fields with ever increasing accuracy of models and theories, the demands on experimental measurement precision and analysis are even greater if new advances are to be made. Such is the case in the mature technology of linear induction accelerators (LIAs) such as the DARHT [1].

More practical considerations also demand uncertainty quantification (UQ) efforts. Multiple measurements techniques may be applied to the same physical quantity at which point a comparison of measurement precision may be decisive. Efforts in this direction include an analysis of the solenoid scan method (*e.g.* Ref. [2]), emittance mask methods [3], or PIC-based analysis of the same experiments [4].

THEORY AND BACKGROUND

Analysis of solenoid scans in LIAs have continuously developed with code capabilities and experimental methods [2, 4]. The most common analysis determines a set of beam initial conditions, upstream of the solenoid magnet being varied, which can then be used to simulate the beam through the remainder of a machine. The beam envelope equation is most relevant to this type of analysis as it includes space-charge effects on the beam; various derivations can be found in the literature [5, 6]. The general form of the envelope equation is given as follows:

$$r_m'' + \frac{\gamma' r_m'}{\beta^2\gamma} + \frac{\gamma'' r_m}{2\beta^2\gamma} + \left(\frac{qB}{2mc\beta\gamma}\right)^2 r_m \cdots - \frac{\epsilon_N^2}{(\beta\gamma)^2 r_m^3} - \frac{K}{r_m} = 0 \quad (1)$$

Leading order effects on the propagation of the beam arise from modifications to the space charge of the beam as might arise from neutralizing of the space charge, current, or ground planes impinged by the beam (e.g. foil focusing [3, 7]).

In beam envelope solutions, the beam edge, a, is associated with the 2 RMS radius of the marginal distribution of the beam. When evaluating the quantities in Eq. (1) at this position, significant corrections are found by inclusion of beam potential depression (BPD). Taking into account this reduction in γ with respect to the beam radius and wall radius creates BPD modifications to Eq. (1) when calculating γ_a' and γ_a''.

Two codes are compared: xtr and simpleEnvelope. The xtr code has been developed over a number of years by personnel at LANL and most physics effects have been validated against experimental measurements. In addition to BPD effects, xtr also takes into account beam diamagnetism effects, which can reduce the effective field of a solenoid magnet by $\approx 1\%$ [8]. A new, python-based code, simpleEnvelope, has been developed to further simulate LIAs with the beam envelope code and enable new modes of analysis. Effects listed above related to space charge and BPD are included in both codes, though simpleEnvelope has not implemented beam diamagnetism.

Analysis of Solenoid Scans

xtr implements an internal profile optimization routine to obtain beam initial radius, divergence, and emittance (R_0, R_0', and ϵ_N) whereas simpleEnvelope is called within a Bayesian framework script: BayesBeam. The xtr solution is obtained by minimizing a χ^2-*like* figure of merit given as:

$$\mathrm{FOM}_{\mathrm{xtr}} = \left[\sum_{i=1}^{N} \frac{\left(r_{\mathrm{meas},i}/r_{t,i} - 1\right)^2}{N}\right]^{1/2} \quad (2)$$

* This work was supported by the U.S. Department of Energy (Contract No. 89233218CNA000001).

ISBN: 978-3-95450-232-5 ISSN: 2673-7000 doi:10.18429/JACoW-NAPAC2022-MOZD4

where N observations are made of the beam radius, $r_{\mathrm{meas},i}$. Variance between the observations and the model solutions, $r_{t,i}$ for a given initial condition set is minimized and reported as the solution. Comparison with the least-squares metric, χ^2 indicates that an equivalence can be drawn via algebraic manipulations *if* one assumes the uncertainty of the observations is equal to the model radii. Uncertainty in the solution parameters is given in terms of the percentage change in a parameter that yields a doubling of $\mathrm{FOM_{xtr}}$. In comparison to a traditional Gaussian distribution, doubling χ strongly reduces the probability of the solution, much more than a single standard deviation, though the exact amount depends on the numerical values of χ^2.

An independent analysis method can be derived using Bayes' rule as follows:

$$p(\mathbf{x}_0|\mathbf{r}_{\mathrm{meas}},\mathbf{I}) = \frac{p(\mathbf{r}_{\mathrm{meas}}|\mathbf{x}_0,\mathbf{I}) \times p(\mathbf{x}_0|\mathbf{I}) \times p(\mathbf{I})}{p(\mathbf{r}_{\mathrm{meas}},\mathbf{I})} \quad (3)$$

where $p(\cdots)$ denotes a probability of the observations for given conditions. A normal distribution is used for the likelihood function given as:

$$p(\mathbf{r}_{\mathrm{meas}}|\mathbf{x}_0,\mathbf{I}) \propto \exp\left[-\frac{1}{2}\left\|\frac{(f(\mathbf{x}_0,\mathbf{I})-\mathbf{r}_{\mathrm{meas}})}{\sigma_{\mathrm{meas}}}\right\|^2\right] \quad (4)$$

where $f(\mathbf{x}_0,\mathbf{I})$ is the beam model solution for the beam initial conditions, $\mathbf{x}_0 = (R_0, R_0', \epsilon_N)$, and machine parameters, $\mathbf{I} = (T_i, I_{b,i}, z_{AM}, \ldots)$ in which we include the measured lab kinetic energy, T_i, measured beam current, $I_{b,i}$, and also allow for anode magnet measurement errors in position, z_{AM}. The machine variable, I_α, where α denotes T, I_b, z_{AM}, etc. is assumed to vary normally.

In single parameter scans, it is possible to utilize a uniform distribution as the prior for $\mathbf{x}_0$. In simulations where lab kinetic energy varies through a distribution, a strong correlation is found with $\mathbf{x}_0$. Strong correlations reduce sampling efficiency so the sampling of the input parameters is made as follows:

$$p(x_\beta, T) = p(x_\beta|T) \times p(T) \quad (5)$$

where we assume a given parameter is distributed as a bivariate normal distribution with T.

APPARATUS AND APPROACH

The experimental apparatus and approach to image acquisition is described in Ref. [3]. Images are taken with a 10 ns gate width centered on the beam pulse. Figure 1 details an example beam envelope solution through the injector region of DARHT-1 when the beam is over-focused by the anode magnet. The OTR images are analyzed to obtain a set of 2 RMS beam radii and uncertainties shown in Fig. 2. This is accomplished by producing a number of marginal distributions through different angular rotations of the image and calculating the RMS size of the beam. This collection of points (24 angles in this work) then provides a mean and standard deviation.

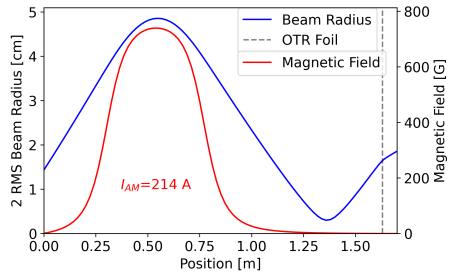

Figure 1: Example beam solution and background magnetic field. The location of the OTR foil is indicated in the figure.

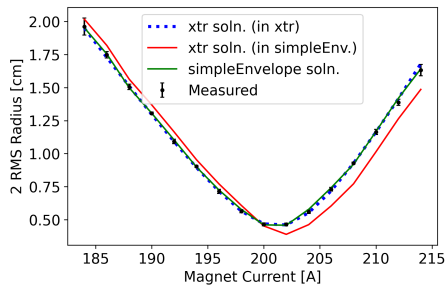

Figure 2: Beam radius vs. anode magnet current for measurements and various model conditions.

The injector voltage on DARHT-1 is monitored by an E-dot probe on each pulse. The E-dot has been cross-calibrated with a permanent magnet spectrometer [9]. The mean kinetic energy during the image acquisition is 3.234 ± 0.006 MeV, though the absolute precision of the cross-calibration yields a 1σ uncertainty of 17 keV. Electron beam current is monitored with a B-dot probe and is found to be 1626 ± 3 A, though here also the absolute precision is estimated to be 0.5% (1σ = 8 A). The location of the beamline components was measured with tape measures and estimated to have a 1σ precision of 1 mm.

The solenoid scans are independently analyzed in both xtr and simpleEnvelope. In the case of xtr, the beam radius for each solenoid excitation is used, without uncertainty estimates. The mean diode voltage and beam current for the entire scan are used. In the case of simpleEnvelope, two cases are considered: case A is a comparison to xtr solution and case B examines the general impact of finite uncertainties. For case A, the mean diode voltage and beam current during the image frame time *for each pulse* as well as the anode magnet position are used and considered known without uncertainty (i.e. $\sigma_T = 0$). For case B, these parameters are allowed to vary.

The xtr code utilizes an optimization algorithm to determine the $\mathbf{x}_0$ that minimizes $\mathrm{FOM_{xtr}}$. Due to the complexity of Eq. (3), in particular the non-linear model function $f(\mathbf{x}_0,\mathbf{I})$, an analytical solution is not available at this time. Instead, the posterior likelihood is solved numerically using a Markov-Chain Monte Carlo sampler. In particular, the PyMC4 library [10] implementation of the Slice algorithm is used to sample the 15 resulting parameters in the model. The model is run using six chains with a burn-in of 2500 draws and 4500 draws.

ISBN: 978-3-95450-232-5 ISSN: 2673-7000 doi:10.18429/JACoW-NAPAC2022-MOZD4

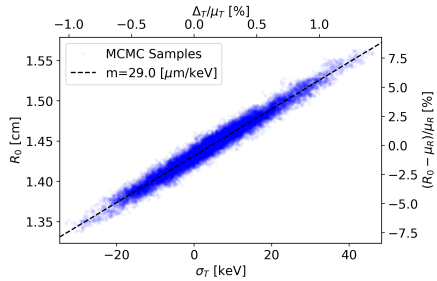

Figure 3: Cross-correlation plot between σ_T and R_0. The covariance between these two variables is found to be 29 µm/keV.

Table 1: Model comparison table showing inferred beam parameters for each xtr and the two simpleEnvelope cases. The reported uncertainty is either the FOM_{xtr} doubling metric or the standard deviation of the posterior distribution.

Model/ Case	R_0 cm	R_0' mrad	ϵ_N mm − mrad
xtr	1.381 ± 0.02	72.6 ± 3.5	957 ± 96
Case (A)	1.432 ± 0.003	72.5 ± 0.5	1132 ± 14
Case (B)	1.445 ± 0.037	72.4 ± 0.5	1137 ± 22

RESULTS AND DISCUSSION

A summary of the analysis results is shown in Table 1. The credible intervals reported are not derived from a fit to the data, but rather calculated directly from the distribution of samples.

Comparing uncertainties between case A and case B, it is clear that the inclusion of energy variation in **I** results in a large increase in uncertainty of the solution. The 1σ value of case B is 370 µm vs. 30 µm in case A. As an illustration of this effect, Fig. 3 shows the cross correlation between the energy variation, σ_T, and the initial radius, R_0. The initial beam radius is found to be most sensitive to this energy variation. This type of range in input beam parameters would have a significant impact on the accelerator transport and matching.

Comparing xtr's solution with case A two points are apparent: that the beam initial conditions vary in a manner that is well beyond the credible intervals and that the uncertainty estimated by xtr exceeds simpleEnvelope by about a factor of 6.5. The difference in solutions is shown in Fig. 2. xtr provides a solution that is consistent with the physics in that model. When this solution is input into the simpleEnvelope code, it no longer closely matches the experimental observations. The solution is displaced by ~2A indicating xtr includes an effect that *weakens* the solenoidal field by about 1% — this is what is expected with beam diagmagnetism. To the second point, a larger uncertainty via the xtr FOM-doubling metric is consistent with the χ^2*-like* interpretation as a doubling of χ would imply a reduced probability far beyond a single standard deviation.

CONCLUSION

A Bayesian analysis for the LIA parameters has been implemented and compared with the established analysis code xtr. The resulting solutions are similar, but distinguishable according to the uncertainties determined by either analysis methodology which we attribute to the lack of beam diamagnetism in the simpleEnvelope code. The solenoid scan method and these analysis techniques, however, provides strong constraints on the inferred solution such that this 1% difference in physics models can be detected. With the inclusion of the finite precision of the absolute calibration, the inferred solution uncertainty grows by an order of magnitude in some cases and indicates new experimental or measurement techniques are needed to better constrain this parameter.

ACKNOWLEDGMENTS

The authors wish to thank the DARHT team for operations support during these experiments as well as P. Allison for many fruitful discussions.

REFERENCES

[1] C. Ekdahl, "Modern Electron Accelerators for Radiography", *IEEE Trans. Plasma Sci.*, vol. 30, pp. 254–261, Feb. 2002. doi:10.1109/ppps.2001.1001997

[2] A. C. Paul, Y.-P. Chong, J. S. Kallman, V. K. Neil, and P. Lee, "Probing the electron distribution inside the ATA beam pulse", *Nucl. Instrum. Methods Phys. Res.*, vol. A300, pp. 137–150, 1991. doi:10.1016/0168-9002(91)90717-5

[3] S. Szustkowski, M. A. Jaworski, and D. C. Moir, "Foil focusing effect in pepper-pot measurements in intense electron beams", *Proc. 13th International Particle Accelerator Conference (IPAC'22)*, Bangkok, 2022, pp. 404–406. doi:10.18429/JACoW-IPAC2022-MOPOPT062

[4] A. F. Press, M. A. Jaworski, D. C. Moir, and S. Szustkowski, "Experimental verification of DARHT Axis 1 injector PIC simulations", *Proc. 13th International Particle Accelerator Conference (IPAC'22)*, Bangkok, 2022, pp. 2183–2185. doi:10.18429/JACoW-IPAC2022-WEPOTK054

[5] E. P. Lee and R. K. Cooper, "General envelope equation for cylindrically symmetric charged-particle beams", *Particle Accelerators*, vol. 7, pp. 83–95, 1976.

[6] M. Reiser, *Theory and Design of Charged Particle Beams*, Weinheim, Germany: Wiley-VCH, 2008. doi:10.1002/9783527622047

[7] R. J. Adler, "Image-field focusing of intense ultra-relativistic electron beams in vacuum", *Particle Accelerators* vol. 12, pp. 39–44, 1982.

[8] P. Allison, "xtr, A New Beam Dynamics Code for DARHT", LANL, Los Alamos, NM, USA, Rep. LA-UR-01-6585, Dec. 2001.

[9] T. J. Burris-Mog, *et al.*, "Calibration of two compact permanent magnet spectrometers for high current electron linear induction accelerators", *Rev. Sci. Instrum.* vol. 89, pp. 073303, 2018. doi:10.1063/1.5029837

[10] J. Salvatier, T.V. Wiecki, and C. Fonnesbeck, "Probabilistic programming in Python using PyMC3", *PeerJ Comp. Sci.* vol. 2, p. e55, 2016. doi:10.48550/arXiv.1507.08050